

Double exchange, itinerant ferromagnetism and topological Hall effect in moiré heterobilayer

Haichen Jia,^{1,*} Bowen Ma,^{1,2,*} Rui Leonard Luo,¹ and Gang Chen^{1,2,†}

¹*Department of Physics and HKU-UCAS Joint Institute for Theoretical and Computational Physics at Hong Kong, The University of Hong Kong, Pokfulam Road, Hong Kong, China*

²*The University of Hong Kong Shenzhen Institute of Research and Innovation, Shenzhen 518057, China*

(Dated: July 21, 2023)

Motivated by the recent experiments and the wide tunability on the MoTe₂/WSe₂ moiré heterobilayer, we consider a physical model to explore the underlying physics for the interplay between the itinerant carriers and the local magnetic moments. In the regime where the MoTe₂ is tuned to a triangular lattice Mott insulator and the WSe₂ layer is doped with the itinerant holes, we invoke the itinerant ferromagnetism from the double exchange mechanism for the itinerant holes on the WSe₂ layer and the local moments on the MoTe₂ layer. Together with the antiferromagnetic exchange on the MoTe₂ layer, the itinerant ferromagnetism generates the scalar spin chirality distribution in the system. We further point out the presence of spin-assisted hopping in addition to the Kondo coupling between the local spin and the itinerant holes, and demonstrate the topological Hall effect for the itinerant electrons in the presence of the non-collinear spin configurations. This work may improve our understanding of the correlated moiré systems and inspire further experimental efforts.

The discovery of the topological and correlation phenomena in the twisted bilayer graphenes has created a new trend of exploring the emergent physics from the moiré lattice and bands on these heterostructure-like platforms [1]. In fact, the fabrication techniques including pulse laser deposition (PLD) and the molecular beam epitaxy (MBE) has been used for a long time to create the heterostructures with layered materials of different physical properties and different degrees of freedom, and modern techniques have been able to fabricate these interfacial heterostructures with the atomic layer precision [2–4]. The unprecedented controllability and manipulability allows these interfaces and heterostructures to access the physical regime and the environment that is absent in the bulk materials and thus host the novel and interesting phenomena [5–8]. Besides the epoch-breaking integer and fractional quantum Hall effects in the semiconductor heterostructures [9, 10], the modern representative emergent phenomena at the heterostructures include the FeSe/SrTiO₃ interfacial superconductivity [11], the Cr-doped Bi₂Se₃ quantum anomalous Hall effect [12], interfacial ferromagnetism and polar catastrophe at the LaAlO₃/SrTiO₃ heterostructure [8, 13] and so on. These results have enriched the scope of topological and correlation physics, and many have inspired the ongoing theoretical development and progress.

In recent years, the transition metal dichalcogenides have attracted significant attention due to the intrinsic spin-orbit coupling, topological bands, valleytronics, valley-selective optics, Ising superconductivity, and the correlation effects [14–16]. The moiré engineering of the transition metal dichalcogenide heterostructures further boosted the field into a new direction [17–19]. The twisted MoTe₂ homobilayers and the MoTe₂/WSe₂ heterobilayers have inspired the more recent interest [20]. In addition to the band structure topology and the fractional quantum Hall states in the twisted MoTe₂ bilayers [21–25], the moiré physics of the MoTe₂/WSe₂ heterobilayer allows more possibilities [26–28]. The layer-dependent electron correlation and the displacement-field-controlled layer electron/hole fillings of the MoTe₂/WSe₂ het-

erobilayer create the bilayer quantum system with both the itinerant electrons and the local moments and allow the study of their self and mutual interactions [26–28]. In the case where the correlated MoTe₂ moiré lattice is filled, one may simulate the triangular lattice Hubbard model and reveal the physics of Mott transition and Mott magnetism [29]. In the case where the itinerant carriers are introduced on the WSe₂ layer, the heavy fermion related physics was identified. On top of these important developments, we explore other emergent physics that may realize on this interesting heterostructure platform.

In the MoTe₂/WSe₂ moiré heterobilayer, it was inferred from the experimental results and the DFT calculations that, the MoTe₂ layer is more correlated than the WSe₂ layer [30]. This is probably because the wavefunctions of the 5*d* electrons from the W atom are more extended than the 4*d* electrons from the Mo atom. The holes in the MoTe₂ layer can be tuned to become local moments, while the holes in the WSe₂ layer can remain itinerant. The heavy fermion type of physics with the Kondo hybridization between the itinerant holes from

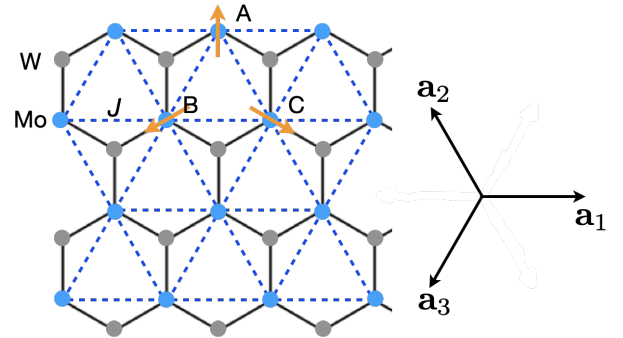


FIG. 1. The moiré Kondo bilayer forms a honeycomb lattice. The moiré sites of the MoTe₂ (WSe₂) layer are labeled by the blue (gray) color. The dashed line refers to the antiferromagnetic exchange coupling between the local moments on the MoTe₂ sites. Here \mathbf{a}_1 , \mathbf{a}_2 , and \mathbf{a}_3 are the three basis vectors of the triangular bravais lattice.

the WSe_2 layer and the local moments from the MoTe_2 layer was observed. To explore the candidate physics, we consider the following Kondo-lattice-like model,

$$H = J \sum_{\langle\langle ij \rangle\rangle_{\text{Mo}}} \mathbf{S}_i \cdot \mathbf{S}_j - t \sum_{\langle\langle ij \rangle\rangle_{\text{W}}} (c_{i\alpha}^\dagger c_{j\sigma} + h.c.) + J_K \sum_{\langle ij \rangle} \mathbf{S}_i \cdot (c_{j\alpha}^\dagger \frac{\sigma_{\alpha\beta}}{2} c_{j\beta}) + \dots, \quad (1)$$

where the J -term is the exchange interaction between the local moments on the Mo layer, the t -term is the hole tunneling on the W layer, the J_K -term is the Kondo coupling between the itinerant hole on the WSe_2 layer and the local moment on the MoTe_2 layer, and the “ \dots ” refers to other interactions such as the spin-assisted hopping of the holes that will be discussed later. The subindex Mo (W) refers to the MoTe_2 (WSe_2) layer. With the “ $1+x$ ” doping, the MoTe_2 moiré sites are occupied by the local magnetic moments, and the remaining x introduces the x hole doping on the WSe_2 moiré sites. As shown in Fig. 1, the moiré lattice of the heterobilayer is a honeycomb lattice. The moiré sites of the MoTe_2 layer form one triangular sublattice, and the moiré sites of the WSe_2 layer form the other triangular sublattice. The operator \mathbf{S}_i refers to the spin-1/2 local moment on the MoTe_2 moiré sites, and $c_{i\alpha}^\dagger$ ($c_{i\alpha}$) creates (annihilates) a hole with spin α at the moiré lattice site i on the WSe_2 layer.

Although the model in Eq. (1) is written with the t and J terms, the physics should differ from the t - J model for the doped Hubbard model where the correlation is uniform throughout the system. For the heterobilayer here, at the current stage, it seems that, the strong Hubbard interaction only occurs on the MoTe_2 moiré sites, but not on the WSe_2 moiré sites. Unlike the t - J model where the hole and the spin exchange each other during the hopping, the hole-hopping only happens on the WSe_2 layer. Therefore, if one attempts to make the connection with the existing physical contexts, the more appropriate one is probably the double exchange model for the doped manganite perovskites with mixed valences of the Mn ions [31–33]. Despite the connection, there still exist some key differences. In the doped manganites, the itinerant carriers from the upper e_g orbitals are on the same lattice sites as the local moments from the lower t_{2g} orbitals, and they interact with a ferromagnetic Hund’s coupling instead of an antiferromagnetic Kondo coupling. Moreover, the parent model for Eq. (1) is actually the Anderson model [34], while the double exchange model is the bare model for the coupling between two species of electrons from the e_g and t_{2g} manifolds.

For the double exchange in doped manganites, the local moment from the t_{2g} orbitals tends to polarize the spin of the itinerant e_g electrons. In the strong Hund’s coupling limit, the spinor wavefunction of the e_g electron is locked to the local moment of each lattice site. When the e_g electron tunnels on the lattice, the overlap of the spinor wavefunctions from neighbor sites determines the effective hopping, and a ferromagnetic spin configuration is preferred in order to gain the

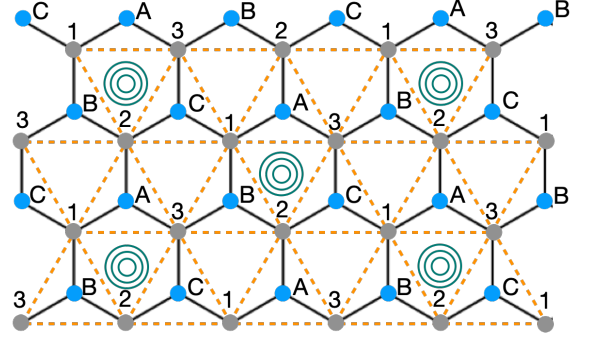


FIG. 2. The sublattices in the presence of the spin-assisted hopping. “1,2,3” refer to the sublattices for the itinerant holes. The enlarged unit cell is labeled by the hexagon plaquette with the marked circle inside.

kinetic energy. When the antiferromagnetic superexchange between the t_{2g} moments is considered, a compromised spin configuration with the spin tilting between the antiferromagnetic order and the collinear ferromagnet is obtained. For the model in Eq. (1), such a ferromagnetic onsite Hund’s coupling is replaced by the antiferromagnetic Kondo coupling from the neighboring sites. Following the spirit of double exchange, the three neighboring spins together polarize the spin of the itinerant hole site at the WSe_2 layer. As the itinerant hole only hops between the moiré sites on the WSe_2 layer, to gain kinetic energy, a ferromagnetic component in the spin configuration would be preferred. Since the Kondo coupling is not as strong as the Hund’s coupling for the manganites, the spinor-charge separation in Zener’s treatment is not directly applicable to the current context to understand the magnetic structure [31]. Instead, we directly consider the total energy of Eq. (1) for the system in the presence of a bit more generic spin configuration.

With only the exchange coupling on the MoTe_2 layer, the ground state of the local moments is simply the 120-degree magnetic order with three sublattices (see Fig. 1). As it is expected to have ferromagnetic components, we then parameterize the spin configuration on the three magnetic sublattices as

$$\langle \mathbf{S}_A \rangle = S(0, \sin \theta, \cos \theta), \quad (2)$$

$$\langle \mathbf{S}_B \rangle = S(-\sqrt{3}(\sin \theta)/2, -(\sin \theta)/2, \cos \theta), \quad (3)$$

$$\langle \mathbf{S}_C \rangle = S(\sqrt{3}(\sin \theta)/2, -(\sin \theta)/2, \cos \theta), \quad (4)$$

where $S = 1/2$, $\theta = 0$ for the fully polarized state, and $\theta = \pi/2$ for the coplanar 120-degree state. One can then single out the itinerant part of the model in Eq. (1) in the presence of the underlying magnetic order, and their contribution is given as

$$\begin{aligned} & -t \sum_{\langle\langle ij \rangle\rangle_{\text{W}}} (c_{i\sigma}^\dagger c_{j\sigma} + h.c.) + \frac{3}{2} S J_K \cos \theta \sum_{i \in \text{W}} c_{j\alpha}^\dagger \sigma_{\alpha\beta}^z c_{j\beta} \\ & = \sum_{\mathbf{k}} \epsilon_+(\mathbf{k}) c_{\mathbf{k}\uparrow}^\dagger c_{\mathbf{k}\uparrow} + \epsilon_-(\mathbf{k}) c_{\mathbf{k}\downarrow}^\dagger c_{\mathbf{k}\downarrow}, \end{aligned} \quad (5)$$

with

$$\epsilon_{\pm}(\mathbf{k}) = -2t \sum_{\mu=1,2,3} \cos(\mathbf{k} \cdot \mathbf{a}_{\mu}) \pm \frac{3}{2} S J_K \cos \theta. \quad (6)$$

Thus, there are two bands that are separated by the ferromagnetic components. In the dilute doping limit, if the hole carriers simply occupy the band bottom of the lower band. Including the exchange energy, the total energy of the system is

$$E_{tot} \simeq (-6t - \frac{3}{2} S J_K \cos \theta) \frac{xN}{2} + \frac{3NJS^2}{4} (3 \cos^2 \theta - 1), \quad (7)$$

where N is the total number of moiré sites. The minimal energy is established for a tilted spin configuration with a finite ferromagnetic component,

$$\cos \theta = \frac{J_K}{6JS} x. \quad (8)$$

A model with the basic ingredients in Eq. (1) is sufficient to generate a weak ferromagnetism via the mechanism of the double exchange. With this spin configuration, the system supports a finite scalar spin chirality within the magnetic unit cell with

$$\chi = \langle (\mathbf{S}_A \times \mathbf{S}_B) \cdot \mathbf{S}_C \rangle \neq 0. \quad (9)$$

Usually, when a finite scalar spin chirality is present in a system with both local moments and itinerant carriers, there should exist a topological Hall effect from the coupling between these two different degrees of freedom. The scalar spin chirality generates a real-space Berry flux for the itinerant carriers, and generates a topological Hall effect by twisting the motion of the carriers. This is absent in the present form of Eq. (1) as the simple Kondo coupling in Eq. (1) does not capture this physics. The itinerant hole experiences the magnetization of the three sublattices as an average, and cannot experience the scalar spin chirality. To obtain the topological Hall effect, one has to return to the parent model, i.e., the Anderson model [34].

The original Anderson model involves the hybridization between the itinerant electron and the local electron orbitals as well the onsite Hubbard- U interaction that creates the local magnetic moment. When one goes from the Anderson model to the Kondo lattice model via the second-order perturbation, in addition to the Kondo coupling between the itinerant carriers and the local moments, there exists a spin-assisted hopping term for the itinerant carriers. From the minimalist's point of view, we consider the following shortest range spin-assisted hopping,

$$\tilde{t} \left[\sum_{\langle\langle ij \rangle\rangle} \sum_{k \in (ij)} (c_{i\alpha}^{\dagger} \sigma_{\alpha\beta} c_{j\beta}) \cdot \mathbf{S}_k + (c_{j\alpha}^{\dagger} \sigma_{\alpha\beta} c_{i\beta}) \cdot \mathbf{S}_k \right], \quad (10)$$

where k is the local moment site in between the sites ij for the itinerant holes. Ideally, it would be better to combine Eq. (10)

and the Eq. (1), and carry out a complete analysis. Here, we take the phenomenological treatment and consider Eq. (10) as a perturbation to Eq. (1) with a small \tilde{t} (compared to J_K). In this approximation, the presence of the spin-assisted hopping in Eq. (10) does not significantly modify the underlying magnetic structure.

With the three-sublattice magnetic order, the unit cell is tripled (see Fig. 2), and the sublattices for the WSe₂ moiré lattice are labeled as "1,2,3". To see the effect of spin-assisted hopping, we simply illustrate the point with one unit cell on the lower left corner of Fig. 2 before performing the actual calculation. Following the treatment of the double exchange theory [31], we first express the electron operator as $c_{i\sigma} = c_i z_{i\sigma}$ where c_i is spinless fermion at i and $z_{i\sigma}$ is the spinor representing the spin state of the itinerant hole. This representation is simply adopted for our physical understanding and cannot be used for our actual calculation. In this representation, the spin-assisted hopping of Eq. (10) becomes

$$\tilde{t} \sum_{\langle\langle ij \rangle\rangle} \sum_{k \in (ij)} [(z_{i\alpha}^* \sigma_{\alpha\beta} z_{j\beta}) c_i^{\dagger} c_j + (z_{j\alpha}^* \sigma_{\alpha\beta} z_{i\beta}) c_j^{\dagger} c_i] \cdot \mathbf{S}_k. \quad (11)$$

If $z_{i\sigma} = z_{j\sigma}$, one should have $z_{i\alpha}^* \sigma_{\alpha\beta} z_{i\beta}$ to be aligned (anti-aligned) with \mathbf{S}_k for $\tilde{t} < 0$ ($\tilde{t} > 0$) to optimize the energy. When the hole hops from 1 to 2, the spin of the hole tends to be aligned with the local moment from the B sublattice. When the hole hops from 2 to 3, the spin of the hole tends to be aligned with the local moment from the C sublattice. When the hole hops from 3 back to 1, the spin of the hole tends to be aligned with the local moment from the A sublattice. Thus, when the hole goes around from 1 to 2 to 3 then to back 1, the spin wavefunction of the hole is twisted from being aligned with the A sublattice order to the B sublattice, then to the C sublattice, and finally back to the A sublattice. Since the spin states are different on the A,B,C sublattices, such a uniform choice of z is frustrated to optimize the energy. This is an example of itinerant frustration. A nonuniform spinor z is generically expected for the 1,2,3 sublattices to optimize the spin-assisted hopping. With the nonuniform z , the original kinetic energy in Eq. (5) becomes

$$-t \sum_{\langle\langle ij \rangle\rangle_w} (z_{i\sigma}^* z_{j\sigma} c_i^{\dagger} c_j + h.c.), \quad (12)$$

where $tz_{i\sigma}^* z_{j\sigma}$ is an effective complex hopping. The complex phase of $tz_{i\sigma}^* z_{j\sigma}$ can then function as an effective U(1) gauge field for the charged spinless fermion. In the context of the double exchange for the doped manganites or the magnetic skyrmion lattices for itinerant magnets, due to the approximate adiabatic condition from the strong *onsite* Hund's coupling, the spinor is pinned by the onsite magnetic order, and the effective U(1) gauge flux is directly related to the solid angle spanned by the noncollinear spin configurations [35, 36]. Here, no such relation is obtained as spin-assisted hopping is a bond coupling term instead of the onsite term, and we are also not really in the adiabatic limit. Although this current process differs from the spinor alignment of the itinerant carriers via

the onsite Kondo/Hund coupling with the local magnetic orders in the context of itinerant magnets, the physical outcome is rather similar. Since the spinor z_i configuration is not expected to be uniform due to the itinerant frustration, the effective real-space U(1) gauge flux is still expected here. Due to the weakness of \tilde{t} and the bond coupling with the spin instead of the onsite coupling, the actual effective flux experienced by the hole is certainly different from the usual expectation from the solid angle spanned by the spins in Eq. (9). Nevertheless, the topological Hall effect of the hole carriers is still expected as well as the resulting momentum space Berry curvature distribution.

In the absence of the spin-assisted hopping, the hole experiences the magnetic order via the off-site Kondo coupling, and the effect is equivalent to a uniform Zeeman coupling because the A,B,C sublattice orders apply to the hole site together and the antiferromagnetic parts are canceled out. Such a Zeeman coupling does not create nontrivial nor finite Berry curvature distribution of the itinerant holes. The spin-assisted hopping transfers the effect of the noncollinear spin texture to the itinerant holes, such that the hole band acquires the Berry curvature distribution in the momentum space. In Fig. 3, we combine Eq. (1) and Eq (10), and explicitly compute dispersion, Berry curvature distribution and Hall conductance for the hole band with the noncollinear spin order as the background. The Hall conductance is given by the Kubo formula [37, 38] as

$$\sigma_H^{xy} = \frac{e^2}{\hbar} \frac{1}{A} \sum_{n,\mathbf{k}} \Theta(\mu - E_{n\mathbf{k}}) \Omega_{n\mathbf{k}}, \quad (13)$$

where A is the area of the xy -plane, μ is the Fermi level determined from doping, Θ is the unit step function as the Fermi-Dirac distribution function at zero-temperature limit, $|n\mathbf{k}\rangle$ ($\langle n\mathbf{k}|$) is the ket (bra)-eigenvector for the n -th folded band, $E_{n\mathbf{k}}$ is its dispersion, and $\Omega_{n\mathbf{k}}$ is the n -th band Berry curvature. After incorporating the three-lattice order, the hole bands are folded into six bands (see Fig. 3). As shown in Fig. 3, the Fermi level μ is just above the band bottom in the dilute doping case, the finite Berry curvature around Γ then indeed leads to a non-zero Hall conductance.

In Eq. (8), we have concluded that a ferromagnetic angle θ can emerge from a simplified consideration, while the interactions of the real materials can make Eq. (8) more complicated, so in Fig. 3 we instead phenomenologically choose a weak ferromagnetic state with $\theta = 83.6^\circ$, and numerically compute the Hall conductance. To explicitly show the effect of the spin-assisted hopping and the spin chirality, in the dilute doping limit, we approximately consider the Berry curvature contribution $\Omega_{1,\mathbf{k}=0} \equiv \Omega_1$ and $\Omega_{2,\mathbf{k}=0} \equiv \Omega_2$ from the band bottom of the two lowest bands, i.e., $E_{1,\mathbf{k}=0} \equiv E_1$ and

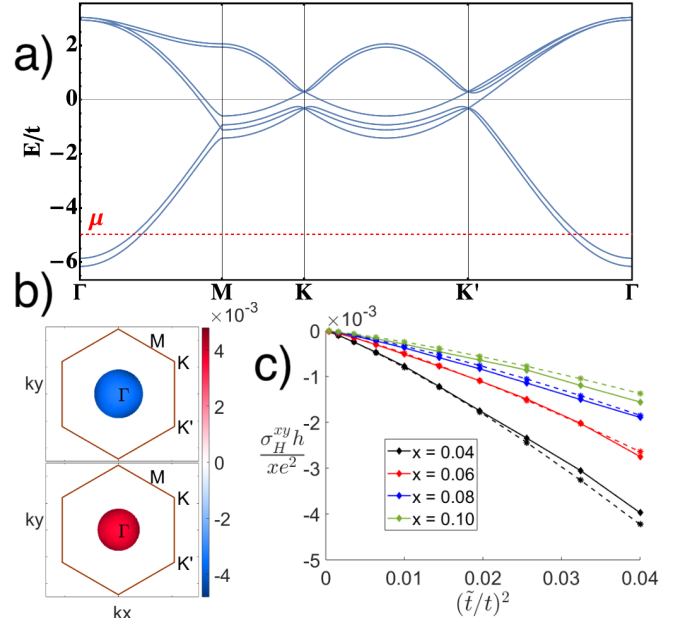


FIG. 3. a) The (folded) band dispersion along high symmetry directions. We choose $\tilde{t} = 0.2t$, $J = 0.3t$, $J_K = t$, with doping $x = 0.1$ and $\theta = 83.6^\circ$. The Fermi level corresponding to $x = 0.1$ is $\mu = -4.96t$ (red dotted line). b) Berry curvature distribution for the states under the Fermi level. Brown hexagon indicates the Brillouin Zone boundary. The upper (lower) part shows the Berry curvature of the lowest (second lowest) band. c) The Hall conductance σ_H^{xy} for various \tilde{t} and filling x , in the unit of $x e^2 / h$. Other parameters are the same as those in (a). Solid lines indicate numerical calculation while dotted lines are computed from analytical estimate Eq. (14).

$E_{2,\mathbf{k}=0} \equiv E_2$ respectively, so that

$$\begin{aligned} \sigma_H^{xy} &\approx \frac{e^2}{\hbar} \frac{Nx}{2A} \frac{(\mu - E_1)\Omega_1 + (\mu - E_2)\Omega_2}{(\mu - E_1) + (\mu - E_2)} \\ &= \frac{e^2}{\hbar} \left\{ \frac{8\pi t(J_K + \tilde{t})}{[9t^2 - (J_K + \tilde{t})^2 S^2 \cos^2 \theta]^2 x} \right. \\ &\quad \left. - \frac{2(J_K + 4\tilde{t}) [9t^2 + (J_K + \tilde{t})^2 S^2 \cos^2 \theta]}{3t [9t^2 - (J_K + \tilde{t})^2 S^2 \cos^2 \theta]^2} \right\} \chi \tilde{t}^2, \quad (14) \end{aligned}$$

where the details of the calculation can be found in the appendix. From this result, it is clear that there is a finite Hall conductance contribution only when the noncollinear spin configuration holds a non-zero spin chirality χ and the Hall conductance is approximately proportional to \tilde{t}^2 , which is consistent with the numerical results in Fig. 3.

Discussion.—The interplay between the itinerant carriers and the local moments in the MoTe₂/WSe₂ moiré heterobilayer reveals the physics of geometric frustration and itinerant frustration that create the noncollinear spin texture and the topological Hall effect via the double exchange mechanism. The current origin of correlation is mainly from the MoTe₂ layer with the moiré triangular lattice. The MoTe₂/WSe₂ moiré heterobilayer has a honeycomb lattice without the inversion symmetry. It will be interesting to increase the cor-

relation on the WSe₂ layer as well such that the system is close to the honeycomb lattice Hubbard model where the inversion symmetry is absent. Since both the interlayer and intralayer coupling/tunneling can be tuned, the system can simulate many rich physics including spiral spin liquid [39, 40], deconfined quantum criticality [41], doped Mott insulator [42] and so on.

Since it has been demonstrated that, the MoTe₂ layer could be tuned from metal to Mott insulator via the Mott transition by more-or-less varying the correlation. Since the antiferromagnetic order appears in the strong Mott regime, this immediately raises the fate of the weak Mott regime where the electron correlation is in the intermediate range. Two possibilities have been discussed. One is the spinon Fermi surface U(1) spin liquid where the spinon sector forms a non-Fermi liquid [43]. In this case, the time-reversal symmetry is preserved, and the interesting direction is to explore the Kondo effect of this spinon non-Fermi liquid with the itinerant carriers. The other one is the chiral spin liquid that was proposed based on the density matrix renormalization group (DMRG) calculation and understood from a recent mean-field study [44, 45]. In this case, the time reversal is broken and there is a chiral edge mode that should support quantized thermal Hall conductance [46]. The coupling of this chiral Abelian topologically ordered state with the itinerant carriers would still generate the topological Hall effect for the itinerant carriers as the scalar spin chirality of the chiral spin liquid can still be experienced by the itinerant carriers. Moreover, the charge-neutral chiral edge mode of the chiral spin liquid may be detected electrically by placing the $C = 1$ chiral edge of integer quantum Hall states on both sides, and such a resonant-tunneling-like idea for the charge-neutral chiral edge mode has been proposed for the (chiral) Kitaev spin liquid and α -RuCl₃ [47]. Here, the MoTe₂/WSe₂ system may be a bit more experimentally feasible as it can naturally support the $C = 1$ quantum Hall state [25].

To summarize, we have explained the itinerant ferromagnetism from the perspective of double exchange and further predicted the topological Hall effect due to the interplay between the itinerant carriers and the local magnetic moments

from the moiré potentials for the MoTe₂/WSe₂ heterobilayer. In addition to these phenomena due to the magnetic orders, the more exotic scenarios were further discussed and visioned.

Acknowledgments.—We acknowledge Kin Fai Mak for the discussion and Wang Yao for the arrangement. This work is supported by the Ministry of Science and Technology of China with Grants No. 2021YFA1400300, the National Science Foundation of China with Grant No. 92065203, and by the Research Grants Council of Hong Kong with C7012-21GF.

APPENDIX A: HAMILTONIAN MATRIX

In this section, we consider the effective Hamiltonian for the itinerant holes at W sites with both Kondo coupling J_K and spin-assisted hopping \tilde{t} as

$$H_W = -t \sum_{\langle\langle ij \rangle\rangle_{w,\sigma}} (c_{i\sigma}^\dagger c_{j\sigma} + h.c.) + J_K \sum_{\langle ij \rangle, \alpha\beta} \mathbf{S}_i \cdot \left(c_{j\alpha}^\dagger \frac{\boldsymbol{\sigma}_{\alpha\beta}}{2} c_{j\beta} \right) + \tilde{t} \left[\sum_{\langle\langle ij \rangle\rangle_w} \sum_{k \in \langle ij \rangle} \sum_{\alpha\beta} \left(c_{i\alpha}^\dagger \boldsymbol{\sigma}_{\alpha\beta} c_{j\beta} + h.c. \right) \cdot \mathbf{S}_k \right], \quad (\text{A1})$$

where the notations are the same as those in the main text. The W sites form a triangular lattice with the six neighboring bonds as $\pm \mathbf{a}_1 = \pm(1, 0)$, $\pm \mathbf{a}_2 = \pm(-1/2, \sqrt{3}/2)$ and $\pm \mathbf{a}_3 = \pm(-1/2, -\sqrt{3}/2)$. Obviously, the non-coplanar “umbrella” spin ordering and the presence of \tilde{t} terms triple the unit cell with three sublattices denoted as 1, 2 and 3. The basis vectors of the enlarged lattice are then $\mathbf{R}_1 = (3/2, -\sqrt{3}/2)$ and $\mathbf{R}_2 = (3/2, \sqrt{3}/2)$. The corresponding reciprocal vectors are $\mathbf{b}_1 = (2\pi/3, -2\pi\sqrt{3}/3)$ and $\mathbf{b}_2 = (2\pi/3, 2\pi\sqrt{3}/3)$.

By performing the Fourier transform in the enlarged lattice, we obtain the Hamiltonian in the basis of $\Psi_{\mathbf{k}} = (c_{1\mathbf{k}\uparrow}, c_{1\mathbf{k}\downarrow}, c_{2\mathbf{k}\uparrow}, c_{2\mathbf{k}\downarrow}, c_{3\mathbf{k}\uparrow}, c_{3\mathbf{k}\downarrow})^T$ as

$$H_W(\mathbf{k}) = \Psi_{\mathbf{k}}^\dagger \begin{bmatrix} \frac{3}{2} J_K S \cos \theta & 0 & f_+(\mathbf{k}) & g_3(\mathbf{k}) & f_+(\mathbf{k}) & g_2(-\mathbf{k}) \\ 0 & -\frac{3}{2} J_K S \cos \theta & g_3^*(-\mathbf{k}) & f_-(\mathbf{k}) & g_2^*(\mathbf{k}) & f_-(\mathbf{k}) \\ f_+^*(\mathbf{k}) & g_3(-\mathbf{k}) & \frac{3}{2} J_K S \cos \theta & 0 & f_+(\mathbf{k}) & g_{1,\mathbf{k}} \\ g_3^*(\mathbf{k}) & f_-^*(\mathbf{k}) & 0 & -\frac{3}{2} J_K S \cos \theta & g_1^*(-\mathbf{k}) & f_-(\mathbf{k}) \\ f_+(\mathbf{k}) & g_2(\mathbf{k}) & f_+^*(\mathbf{k}) & g_1(-\mathbf{k}) & \frac{3}{2} J_K S \cos \theta & 0 \\ g_2^*(-\mathbf{k}) & f_-(\mathbf{k}) & g_{1,\mathbf{k}} & f_-^*(\mathbf{k}) & 0 & -\frac{3}{2} J_K S \cos \theta \end{bmatrix} \Psi_{\mathbf{k}}, \quad (\text{A2})$$

where $f_\sigma(\mathbf{k}) = -(t - \sigma \tilde{t} S \cos \theta) \sum_{\mu=1,2,3} e^{-i\mathbf{k} \cdot \mathbf{a}_\mu}$ and $g_n(\mathbf{k}) = -i \tilde{t} S \sin \theta \sum_{\mu=1,2,3} e^{-i[\mathbf{k} \cdot \mathbf{a}_\mu - \frac{2\pi}{3}(\mu+n)]}$. By diagonalizing the matrix in Eq. (A2), we obtain the band dispersion

as shown in Fig. 3 in the main text.

APPENDIX B: HALL CONDUCTANCE ESTIMATE

In this section, we analytically calculate the Hall conductance in the dilute doping limit. In this case, most related physics can be captured in the energy region between the band bottom and the chemical potential μ . Since t and $J_K > 0$, when $|\tilde{t}| \ll J_K$, the band bottom occurs at Γ point, i.e. $\mathbf{k} = (0, 0)$. Fortunately, an exact diagonalization of Eq. (A2) can be achieved at Γ , and the two lowest energies are

$$E_{1,2} = -6t \mp \frac{3}{2}S \cos \theta (J_K + 4\tilde{t}). \quad (\text{B1})$$

When $\tilde{t} = 0$, the lowest energy E_1 recovers Eq. (6) in the main text, and small \tilde{t} indeed only affects θ perturbatively.

Moreover, we can analytically calculate the Berry curvature of these two bands at Γ as

$$\Omega_{1,2} = \mp \frac{3S^2 \tilde{t}^2 \sin^2 \theta}{2 [3t \pm (J_K + \tilde{t})S \cos \theta]^2}. \quad (\text{B2})$$

Approximately,

$$\begin{aligned} \sigma_H^{xy} &\approx \frac{e^2}{\hbar A_0} \left[\Omega_1 \int \frac{d^2 \mathbf{k}}{(2\pi)^2} f(E_{1\mathbf{k}}) + \Omega_2 \int \frac{d^2 \mathbf{k}}{(2\pi)^2} f(E_{2\mathbf{k}}) \right] \\ &= \frac{e^2}{2\pi \hbar A_0} \left[\Omega_1 \int_{E_1}^{\mu} dE \frac{d^2 \mathbf{k}}{dE_{1\mathbf{k}}} + \Omega_2 \int_{E_2}^{\mu} dE \frac{d^2 \mathbf{k}}{dE_{2\mathbf{k}}} \right], \end{aligned} \quad (\text{B3})$$

where $A_0 = \frac{\sqrt{3}}{2}$ is the area per W sites.

Again, since $|\tilde{t}| \ll J_K$, we estimate $\frac{d^2 \mathbf{k}}{dE_{1(2),\mathbf{k}}}$ using the dispersion relation at $\tilde{t} = 0$, i.e. $\epsilon_{\pm}(\mathbf{k}) = -2t \sum_{\mu} \cos(\mathbf{k} \cdot \mathbf{a}_{\mu}) \pm \frac{3}{2}J_K S \cos \theta \approx \frac{3}{2}t|\mathbf{k}|^2 - 6t \pm \frac{3}{2}J_K S \cos \theta$, to get $\frac{d^2 \mathbf{k}}{dE_{1(2),\mathbf{k}}} \approx \frac{d^2 \mathbf{k}}{d\epsilon_{\pm,\mathbf{k}}} \approx \frac{2\pi}{3t}$.

We can also estimate μ from x -doping as

$$\begin{aligned} x &= \int_{E_1}^{\mu} \frac{dE}{(2\pi)^2} \frac{d^2 \mathbf{k}}{dE_{1\mathbf{k}}} + \int_{E_2}^{\mu} \frac{dE}{(2\pi)^2} \frac{d^2 \mathbf{k}}{dE_{2\mathbf{k}}} \\ &\approx \frac{\mu - E_1}{6\pi t} + \frac{\mu - E_2}{6\pi t} = \frac{\mu + 6t}{3\pi t}, \end{aligned} \quad (\text{B4})$$

or alternatively,

$$\mu = 3(\pi x - 2)t \quad (\text{B5})$$

Then,

$$\begin{aligned} \sigma_H^{xy} &\approx \frac{e^2}{\hbar A_0} \left(\Omega_1 \frac{\mu - E_1}{3t} + \Omega_2 \frac{\mu - E_2}{3t} \right) \\ &= \frac{e^2}{\hbar} \sqrt{3} S^2 \tilde{t}^2 \sin^2 \theta \left\{ \frac{\pi x - \frac{(J_K + 4\tilde{t})S \cos \theta}{2t}}{[3t - (J_K + \tilde{t})S \cos \theta]^2} - \frac{\pi x + \frac{(J_K + 4\tilde{t})S \cos \theta}{2t}}{[3t + (J_K + \tilde{t})S \cos \theta]^2} \right\} \\ &= \frac{e^2}{\hbar} \frac{12\pi t^2 (J_K + \tilde{t})x - (J_K + 4\tilde{t}) [9t^2 + (J_K + \tilde{t})^2 S^2 \cos^2 \theta]}{t [9t^2 - (J_K + \tilde{t})^2 S^2 \cos^2 \theta]^2} \frac{2}{3} \chi \tilde{t}^2 \end{aligned} \quad (\text{B6})$$

which is proportional to spin chirality χ and \tilde{t}^2 .

* These authors contributed equally to this work.

† ganchen@hku.hk

- [1] Eva Y. Andrei and Allan H. MacDonald, “Graphene bilayers with a twist,” *Nature Materials* **19**, 1265–1275 (2020).
- [2] J. D. Ferguson, G. Arikian, D. S. Dale, A. R. Woll, and J. D. Brock, “Measurements of surface diffusivity and coarsening during pulsed laser deposition,” *Phys. Rev. Lett.* **103**, 256103 (2009).
- [3] J. Mannhart and D. G. Schlom, “Oxide interfaces—an opportunity for electronics,” *Science* **327**, 1607 (2010).
- [4] Naoyuki Nakagawa, Harold Hwang, and David Muller, “Why

some interfaces cannot be sharp,” *Nature Materials* **5**, 204–209 (2006).

- [5] Jak Chakhalian, Andrew J Millis, and James M Rondinelli, “Whither the oxide interface,” *Nature materials* **11**, 92–94 (2012).
- [6] Harold Y Hwang and Y Iwasa, “Emergent phenomena at oxide interfaces,” *Nature materials* **11**, 103–113 (2012).
- [7] S Thiel, G Hammerl, A Schmehl, CW Schneider, and J Mannhart, “Tunable quasi-two-dimensional electron gases in oxide heterostructures,” *Science* **313**, 1942–1945 (2006).
- [8] A. Ohtomo and H.Y. Hwang, “A high-mobility electron gas at the LaAlO₃/SrTiO₃ heterointerface,” *Nature* **427**, 423–426 (2004).
- [9] K von Klitzing, G Dorda, and M Pepper, “New method for high-accuracy determination of the fine-structure constant based on quantized Hall resistance,” *Physical review letters* **45**,

- 494–497 (1980).
- [10] D. C. Tsui, H. L. Stormer, and A. C. Gossard, “Two-dimensional magnetotransport in the extreme quantum limit,” *Phys. Rev. Lett.* **48**, 1559–1562 (1982).
- [11] Qing-Yan Wang, Zhi Li, Wen-Hao Zhang, Zhi-Chen Zhang, Jun-Sen Zhang, Wei Li, Hao Ding, Yun-Bo Ou, Peng Deng, Kai Chang, *et al.*, “Interface-induced high-temperature superconductivity in single unit-cell FeSe films on SrTiO₃,” *Chinese Physics Letters* **29**, 037402 (2012).
- [12] C-Z Chang, J Zhang, X Feng, J Shen, Z Zhang, M Guo, K Li, Y Ou, P Wei, L-L Wang, *et al.*, “Experimental observation of the quantum anomalous Hall effect in a magnetic topological insulator,” *Science* **340**, 167–170 (2013).
- [13] Lu Li, Curt Richter, Jochen Mannhart, and Raymond C Ashoori, “Coexistence of magnetic order and two-dimensional superconductivity at LaAlO₃/SrTiO₃ interfaces,” *Nature Physics* **7**, 762–766 (2011).
- [14] S. Manzeli, D. Ovchinnikov, D. Pasquier, O V Yazyev, and A. Kis, “2D transition metal dichalcogenides,” *Nature Reviews Materials* **2**, 17033 (2017).
- [15] Dmitry K. Efimkin and Allan H. MacDonald, “Correlation physics in transition metal dichalcogenides,” *Reports on Progress in Physics* **81**, 056503 (2018).
- [16] Ting Cao, Yue Zhao, and Steven G Louie, “Topological phases in two-dimensional materials: a review,” *Reports on Progress in Physics* **81**, 026501 (2018).
- [17] Qiyuan Wang, Hongqian Xie, Xiaojun Li, Hua Zhang, and Yong-Wei Zhang, “Emerging properties of two-dimensional transition metal dichalcogenides heterostructures,” *Chemical Society Reviews* **47**, 6101–6127 (2018).
- [18] K S Novoselov, A Mishchenko, A Carvalho, and AH Castro Neto, “2D materials and van der Waals heterostructures,” *Science* **353**, aac9439 (2016).
- [19] A.K. Geim and I.V. Grigorieva, “Van der Waals heterostructures,” *Nature* **499**, 419–425 (2013).
- [20] Kyle L Seyler, Pasqual Rivera, Hongyi Yu, Nathan P Wilson, Eric L Ray, David G Mandrus, Jiaqiang Yan, Wang Yao, and Xiaodong Xu, “Signatures of moiré-trapped valley excitons in MoSe₂/WSe₂ heterobilayers,” *Nature* **567**, 66–70 (2019).
- [21] Fengcheng Wu, Timothy Lovorn, Emanuel Tutuc, Ivar Martin, and A. H. MacDonald, “Topological insulators in twisted transition metal dichalcogenide homobilayers,” *Phys. Rev. Lett.* **122**, 086402 (2019).
- [22] Eric Anderson, Feng-Ren Fan, Jiaqi Cai, William Holtzmann, Takashi Taniguchi, Kenji Watanabe, Di Xiao, Wang Yao, and Xiaodong Xu, “Programming Correlated Magnetic States via Gate Controlled Moiré Geometry,” (2023), [arXiv:2303.17038](https://arxiv.org/abs/2303.17038) [[cond-mat.mes-hall](https://arxiv.org/abs/2303.17038)].
- [23] Jiaqi Cai, Eric Anderson, Chong Wang, Xiaowei Zhang, Xiaoyu Liu, William Holtzmann, Yinong Zhang, Fengren Fan, Takashi Taniguchi, Kenji Watanabe, Ying Ran, Ting Cao, Liang Fu, Di Xiao, Wang Yao, and Xiaodong Xu, “Signatures of Fractional Quantum Anomalous Hall States in Twisted MoTe₂,” *Nature* (2023), [10.1038/s41586-023-06289-w](https://doi.org/10.1038/s41586-023-06289-w).
- [24] Yihang Zeng, Zhengchao Xia, Kaifei Kang, Jiacheng Zhu, Patrick Knüppel, Chirag Vaswani, Kenji Watanabe, Takashi Taniguchi, Kin Fai Mak, and Jie Shan, “Integer and fractional Chern insulators in twisted bilayer MoTe₂,” (2023), [arXiv:2305.00973](https://arxiv.org/abs/2305.00973) [[cond-mat.mes-hall](https://arxiv.org/abs/2305.00973)].
- [25] Zui Tao, Bowen Shen, Shengwei Jiang, Tingxin Li, Lizhong Li, Liguang Ma, Wenjin Zhao, Jenny Hu, Kateryna Pistunova, Kenji Watanabe, Takashi Taniguchi, Tony F. Heinz, Kin Fai Mak, and Jie Shan, “Valley-coherent quantum anomalous Hall state in AB-stacked MoTe₂/WSe₂ bilayers,” (2022), [arXiv:2208.07452](https://arxiv.org/abs/2208.07452) [[cond-mat.mes-hall](https://arxiv.org/abs/2208.07452)].
- [26] Wenjin Zhao, Bowen Shen, Zui Tao, Zhongdong Han, Kaifei Kang, Kenji Watanabe, Takashi Taniguchi, Kin Fai Mak, and Jie Shan, “Gate-tunable heavy fermions in a moiré Kondo lattice,” *Nature* **616**, 61–65 (2023).
- [27] Kaifei Kang, Wenjin Zhao, Yihang Zeng, Kenji Watanabe, Takashi Taniguchi, Jie Shan, and Kin Fai Mak, “Switchable moiré potentials in ferroelectric WTe₂/WSe₂ superlattices,” (2022), [arXiv:2209.04981](https://arxiv.org/abs/2209.04981) [[cond-mat.mes-hall](https://arxiv.org/abs/2209.04981)].
- [28] Yang Xu, Kaifei Kang, Kenji Watanabe, Takashi Taniguchi, Kin Fai Mak, and Jie Shan, “A tunable bilayer hubbard model in twisted WSe₂,” *Nature Nanotechnology* **17**, 934–939 (2022).
- [29] Tingxin Li, Shengwei Jiang, Lizhong Li, Yang Zhang, Kaifei Kang, Jiacheng Zhu, Kenji Watanabe, Takashi Taniguchi, Debanjan Chowdhury, Liang Fu, Jie Shan, and Kin Fai Mak, “Continuous Mott transition in semiconductor moiré superlattices,” *Nature* **597**, 350–354 (2021).
- [30] Yang Zhang, Trithep Devakul, and Liang Fu, “Spin-textured chern bands in AB-stacked transition metal dichalcogenide bilayers,” *Proceedings of the National Academy of Sciences* **118** (2021), [10.1073/pnas.2112673118](https://doi.org/10.1073/pnas.2112673118).
- [31] Clarence Zener, “Interaction between the *d*-Shells in the Transition Metals. II. Ferromagnetic Compounds of Manganese with Perovskite Structure,” *Phys. Rev.* **82**, 403–405 (1951).
- [32] P. G. de Gennes, “Effects of Double Exchange in Magnetic Crystals,” *Physical Review* **118**, 141–154 (1960).
- [33] Maria Azhar and Maxim Mostovoy, “Incommensurate spiral order from double-exchange interactions,” *Phys. Rev. Lett.* **118**, 027203 (2017).
- [34] Alexander Cyril Hewson, *The Kondo Problem to Heavy Fermions*, Cambridge Studies in Magnetism (Cambridge University Press, 1993).
- [35] Jinwu Ye, Yong Baek Kim, A. J. Millis, B. I. Shraiman, P. Majumdar, and Z. Tešanović, “Berry Phase Theory of the Anomalous Hall Effect: Application to Colossal Magnetoresistance Manganites,” *Phys. Rev. Lett.* **83**, 3737–3740 (1999).
- [36] Takashi Kurumaji, Taro Nakajima, Max Hirschberger, Akiko Kikkawa, Yuichi Yamasaki, Hajime Sagayama, Hironori Nakao, Yasujiro Taguchi, Taka hisa Arima, and Yoshinori Tokura, “Skyrmion lattice with a giant topological hall effect in a frustrated triangular-lattice magnet,” *Science* **365**, 914–918 (2019).
- [37] Ryogo Kubo, “Statistical-mechanical theory of irreversible processes. i. general theory and simple applications to magnetic and conduction problems,” *Journal of the physical society of Japan* **12**, 570–586 (1957).
- [38] D. J. Thouless, M. Kohmoto, M. P. Nightingale, and M. den Nijs, “Quantized hall conductance in a two-dimensional periodic potential,” *Phys. Rev. Lett.* **49**, 405–408 (1982).
- [39] A. Mulder, R. Ganesh, L. Capriotti, and A. Paramekanti, “Spiral order by disorder and lattice nematic order in a frustrated heisenberg antiferromagnet on the honeycomb lattice,” *Phys. Rev. B* **81**, 214419 (2010).
- [40] Xu-Ping Yao, Jian Qiao Liu, Chun-Jiong Huang, Xiaoqun Wang, and Gang Chen, “Generic spiral spin liquids,” *Frontiers of Physics* **16** (2021), [10.1007/s11467-021-1074-9](https://doi.org/10.1007/s11467-021-1074-9).
- [41] R. Ganesh, Jeroen van den Brink, and Satoshi Nishimoto, “Deconfined Criticality in the Frustrated Heisenberg Honeycomb Antiferromagnet,” *Phys. Rev. Lett.* **110**, 127203 (2013).
- [42] Zheng-Cheng Gu, Hong-Chen Jiang, D. N. Sheng, Hong Yao, Leon Balents, and Xiao-Gang Wen, “Time-reversal symmetry breaking superconducting ground state in the doped Mott insulator on the honeycomb lattice,” *Phys. Rev. B* **88**, 155112 (2013).

- [43] Sung-Sik Lee and Patrick A. Lee, “U(1) Gauge Theory of the Hubbard Model: Spin Liquid States and Possible Application to κ -(BEDT-TTF)₂Cu₂(CN)₃,” *Phys. Rev. Lett.* **95**, 036403 (2005).
- [44] Aaron Szasz, Johannes Motruk, Michael P. Zaletel, and Joel E. Moore, “Chiral Spin Liquid Phase of the Triangular Lattice Hubbard Model: A Density Matrix Renormalization Group Study,” *Phys. Rev. X* **10**, 021042 (2020).
- [45] Tessa Cookmeyer, Johannes Motruk, and Joel E. Moore, “Four-spin terms and the origin of the chiral spin liquid in mott insulators on the triangular lattice,” *Phys. Rev. Lett.* **127**, 087201 (2021).
- [46] Xiao-Tian Zhang, Yong Hao Gao, and Gang Chen, “Thermal hall effects in quantum magnets,” (2023), [arXiv:2305.04830 \[cond-mat.str-el\]](https://arxiv.org/abs/2305.04830).
- [47] David Aasen, Roger S. K. Mong, Benjamin M. Hunt, David Mandrus, and Jason Alicea, “Electrical Probes of the Non-Abelian Spin Liquid in Kitaev Materials,” *Phys. Rev. X* **10**, 031014 (2020).